Gradient galectin-1 coating technology: bionic multichannel nerve guidance conduits promote neural cell migration

RESEARCH ARTICLE

Gradient galectin-1 coating technology: bionic multichannel nerve guidance conduits promote neural cell migration

Na Liu[1, #], Xuchao Ning[2, #], Xiaopei Zhang[1, 2, 3], Ziyi Zhou[1, 2], Manfei Fu[4], Yuanfei Wang[5, *], Tong Wu[1, 2, 3, *]

1 Institute of Neuroregeneration & Neurorehabilitation, Department of Pathophysiology, School of Basic Medicine, Qingdao University, Qingdao, Shandong Province, China

2 The Affiliated Hospital of Qingdao University, Qingdao Medical College, Qingdao University, Qingdao, Shandong Province, China

3 Shandong Key Laboratory of Medical and Health Textile Materials, Collaborative Innovation Center for Eco-textiles of Shandong Province and the Ministry of Education, College of Textiles & Clothing, Qingdao University, Qingdao, Shandong Province, China

4 School of Pharmacy, University of Reading, Whiteknights, UK

5 Qingdao Stomatological Hospital Affiliated to Qingdao University, Qingdao, Shandong Province, China

#These authors contributed equally to this work.

*Correspondence to: Yuanfei Wang, PhD, zhizunbao19@163.com; Tong Wu, PhD, twu@qdu.edu.cn.

orcid: 0000-0003-4134-307X (Yuanfei Wang); 0000-0001-8822-1868 (Tong Wu)

Abstract

Engineered nerve guidance conduits have been widely used to repair peripheral nerve injuries. Galectin-1 is an important biological cue that promotes axon regeneration and Schwann cell migration. In this study, a series of polycaprolactone-based nerve guidance conduits were prepared. First, we determined the concentration of galectin-1 (a member of the galactose lectin family) via the proliferation and morphology of Schwann cells and the viability, morphology, and axon length of PC12 cells. On this basis, nanofiber yarns coated with a uniform or unidirectionally linear gradient coating layer of galectin-1 were prepared by electrospinning to investigate the viability and migration of Schwann cells and neural stem cells on the surfaces. The unidirectional linear gradient coating with increasing galectin-1 content was found to promote the migration of both Schwann cells and neural stem cells. To construct nerve guidance conduits with encapsulated nanofiber yarns, we fabricated nerve guidance conduit walls composed of conjugately electrospun nanofiber yarns and random polycaprolactone nanofibers as the inner and outer layers. With a biocompatible light-absorbing dye, the nanofibers can be sealed via light welding to obtain a hollow polycaprolactone conduit. Finally, we prepared nerve guidance conduits containing nanofiber yarns coated with graded galectin-1 as well as hyaluronic acid methacryloyl hydrogel in the lumen. We found that the topology (nanofiber yarns and hyaluronic acid methacryloyl) and biological cues (gradient galectin-1 coating) synergistically accelerated the migration of Schwann cells and neural stem cells along multiple channels of nerve guidance conduits.

Key words: biological cues; biomaterials; galectin-1; gradient coating; nanofiber yarns; nerve guidance conduit; neural stem cells; neural tissue engineering; synergistic effect; Schwann cells; technology; technique; topology

doi: 10.4103/ATN.ATN-D-24-00010

Funding: This study was supported by the Special Funds for Taishan Scholars Project of Shandong Province, No. tsqn202211125; the Natural Science Foundation of Shandong Province, No. ZR2021YQ17; and the Young Elite Scientists Sponsorship Program by CAST, No. YESS20200097.

How to cite this article: Liu N, Ning X, Zhang X, Zhou Z, Fu M, Wang Y, Wu T. Gradient galectin-1 coating technology: bionic multichannel nerve guidance conduits promote neural cell migration. Adv Technol Neurosci. 2024;1(2):276-289.

INTRODUCTION

Peripheral nerve injury (PNI) is a common neurosurgical disease that is caused mainly by trauma and has high morbidity and disability rates, which affect patients' quality of life. In addition, limb hyperextension, fracture and dislocation, diabetes, and improper drug injection can also lead to peripheral nerve damage. Currently, PNI is often treated clinically via nerve grafting, but allografts and xenografts can trigger an immune reaction, leading to surgical failure.[1] Autologous nerve grafts, in turn, can lead to damage and loss of function in other normal tissues.[2] Therefore, there is an urgent need to develop new alternative strategies, and the primary issues to be addressed are immune rejection-free, tension-free, and end-to-end repair. Neural tissue engineering plays an important role in the repair and regeneration of PNI, especially in the development and design of biomaterial-based nerve guidance conduits (NGCs) that increasingly conform to the human structure and are expected to allow more efficient replacement of autologous nerves.[3, 4]

NGCs are usually applied to bridge nerve severance sites, providing a suitable microenvironment for nerve

regeneration and restoring impaired motor and sensory function.[5] To date, some NGCs have been approved by the U.S. Food and Drug Administration to repair clinical nerve defects. However, most hollow NGCs approved by the U.S. Food and Drug Administration are suitable only for short lesions, which are poorly permeable and undirected, leading to poor neurological recovery.[6] Recently, studies have shown that multichannel or filled NGCs with oriented microstructures can effectively improve the regeneration ability and functional recovery of nerve cells at injured sites. For example, the preparation of conductive multiscale-filled NGCs with layered-oriented fibers via three-dimensional (3D) printing technology can significantly enhance peripheral nerve regeneration.[7] A series of multichannel conduits have been proven to be structures conducive to peripheral nerve regeneration.[8] Some improved electrospinning methods have been used to prepare nanofiber yarns to induce the proliferation and migration of nerve cells in neural tissue engineering. A filled nerve conduit was fabricated using poly(lactic-co-glycolic acid) nanofiber yarns in the lumen and laminin-coated poly(lactic-co-glycolic acid) fibers as the tube wall.[9] The results showed that the nanofiber yarns of such bionic nerve fiber bundles could regulate Schwann cell (SC) migration. Therefore, it is necessary to integrate the advantages of existing types of NGCs and synergize the topology and biological cues of biomaterials to construct multiscale bionic NGCs.[10]

Polycaprolactone (PCL) is commonly used as a cell growth support material because of its good biocompatibility, biodegradability, and high mechanical strength.[11] PCL is widely used for electrospinning to prepare oriented or random nanofibers for different research purposes, such as the repair of nerves, skin, bone, and tendons.[12, 13] In addition, electrospinning can also load biochemical cues, such as various biological proteins, drugs, and chemicals, which can work synergistically in conjunction with the unique topology of the scaffold materials. Researchers have reported that galectin-1, a member of the galactose lectin family, has a wide range of biological functions and is involved in many processes, including immunity, inflammation, nervous system development, and skeletal muscle growth.[14] The reduction and oxidation states of galectin-1 have specific positive effects on repairing damaged nerves.[15, 16] Data from *in vivo* and *in vitro* neural regeneration models indicate that the oxidation state of galectin-1 (galectin-1/Ox) promotes axon regeneration.[17] Preclinical studies have demonstrated that galectin-1/Ox at the surgical site can restore neurological function.[18] Local administration of galectin-1/Ox can also promote the migration of SCs at the proximal and distal ends of nerve fractures, accelerating the regeneration of motor and sensory nerves, even in allografts.[19] In conclusion, galectin-1 is a compelling biological clue that promotes axon regeneration and SC migration.

Combining topography and biological signals through electrospray allows a gradient biological signal of galectin-1 to guide the directional migration of nerve repair-related cells, which is beneficial for promoting the repair of PNI.[20] Hyaluronic acid methacryloyl (HAMA) can be crosslinked and cured under ultraviolet light as an injectable photosensitive biomaterial to achieve a stable structure.[21] In addition, it also has excellent biocompatibility and inhibits inflammation and other effects.[22] These advantages have been applied in many biomedical research fields, e.g., controlled drug release, nerve conduit preparation, wound dressing, and postoperative antiadhesion.[23] Refinement of the NGC wall and lumen includes continuous optimization of topology, biochemical cues, and other interactions that provide NGCs with features that promote neural repair, such as directed axon growth, neural stem cell (NSC) and SC migration, and phenotype expression.[24-26] This study developed a novel NGC (NGCs containing nanofiber yarns coated with gradient galectin-1 and HAMA hydrogel) via double-nozzle electrospinning, traditional electrospinning, and electrospray technologies. The viability, distribution, and migration of NSCs and SCs on the nanofiber yarns and the nanofiber yarns coated with uniform or gradient galectin-1 were evaluated. The potential applications of H-PCL NGCs, NGCs containing nanofiber yarns (NY-PCL NGCs), NGCs containing nanofiber yarns coated with gradient galectin-1 (GC-NY-PCL NGCs), and HA-GC-NY-PCL NGCs in neural tissue engineering were also explored.

METHODS

Materials

Hexafluoroisopropanol (HFIP), rhodamine B, and acetic acid were purchased from Macklin (Shanghai, China). PCL (Mw ≈ 80,000 g/mol) and porcine skin type I gelatin were supplied by Sigma–Aldrich (St. Louis, MO, USA). Indocyanine green (ICG), Dulbecco's modified Eagle's medium (DMEM), antibiotic-antimycotic, and 4',6-diamidino-2-phenylindole (DAPI) were acquired from Solarbio (Beijing, China). Phalloidin-iFluor 488 was obtained from Abcam (UK, Cambridge). Fetal bovine serum (FBS) was purchased from Pan (Bonn, Germany). A Cell Counting Kit-8 (CCK-8) was purchased from NCM Biotech (Suzhou, China). A neurite outgrowth staining kit was purchased from Thermo Fisher Scientific (Shanghai, China). Recombinant human galectin-1

was purchased from PeproTech Company (Suzhou, China). SCs (rat), NSCs (rat), and PC12 cells (rat adrenal pheochromocytoma cells) were kindly provided by the Advanced Biomaterials and Regenerative Medicine (ABRM) group of Qingdao University. The cell lines used in this study were commercially available, and ethical approval was waived.

Determination of the concentration of galectin-1

Schwann cellproliferation and morphology

With reference to galectin-1 concentrations mentioned in previous studies, three experimental groups were designed: 5, 20, and 50 ng/mL.[17, 19, 27, 28] The SCs were inoculated in 24-well plates at a concentration of 5 × 10^3 cells/well, and 500 µL of DMEM containing 1% FBS was added to the control group (n = 3). The effects of different galectin-1 concentrations on SC proliferation were detected via the CCK-8 method on days 1, 3, and 5. At each time, the medium was removed from the wells, and fresh complete medium containing 10% CCK-8 reagent was added. After incubation at 37°C for 3 hours, the absorbance of the supernatant at 450 nm was measured with an enzyme-labeled instrument.

The cells from day 3 were fixed and stained with Phalloidin-iFluor 488 dye and DAPI to observe the effects of different concentrations of galectin-1 on cell morphology. The procedures included removing the medium from each well, washing the samples twice with PBS, and fixing the cells with 4% paraformaldehyde at room temperature for 30 minutes. After the paraformaldehyde was removed, the samples were washed with PBS three times and then treated with 0.1% Triton X-100 for 5 minutes. Afterward, the samples were treated with 1% bovine serum albumin solution for 1 hour. Phalloidin-iFluor 488 dye was mixed with 1% bovine serum albumin solution at a ratio of 1:1000, and 200 µL of the dye mixture was added to each well. After the samples were incubated at room temperature for 30 minutes in the dark, DAPI was added to stain the nuclei.

PC12 cell viability and axon staining assay

PC12 cells can exhibit a phenotype similar to that of neuronal cells, with varying numbers of protrusions and long synapses resembling neuronal axons, making them suitable for axonal growth studies.[29] PC12 cells were cultured with different concentrations of galectin-1. Briefly, PC12 cells were inoculated in 24-well plates at a concentration of 2 × 10^3 cells/well, and the control group was treated with 500 µL of DMEM containing 1% FBS. The growth of the PC12 cells was observed daily under a microscope. After 4 days of culture, the effects of different concentrations of galectin-1 on the viability of PC12 cells were detected via the CCK-8 method. Moreover, the axons were stained, and the length of the PC12 axons in each group was subsequently determined via ImageJ software (version 2024; National Institutes of Health, Bethesda, MD, USA).

Preparation and characterization of the nanofibers

PCL was dissolved in HFIP at 12% (w/v) and stirred overnight with a magnetic stirrer. The uniaxially aligned nanofibers were fabricated via traditional electrospinning, conjugate nanofiber yarns (NFY-1) via double-nozzle electrospinning, and the nanofiber yarns (NFY-2) were produced via a commercial instrument.[30, 31] The parameters for uniaxially aligned nanofibers were as follows: high voltage of 10.5 kV, flow rate of 1 mL/h, receiving distance of 15 cm, and collection time of 2 hours. The parameters for NFY-1 were as follows: high voltage of 12 kV, flow rate of 1 mL/h for two needles in opposite directions, distance between the two needles of 15 cm, distance between the needles and the rotating collector (130 r/min) of 20 cm, and collection time of 2 hours. The parameters for NFY-2 were as follows: high voltage of 9.8 kV, flow rate of 0.02 mL/min for two spinnerets in opposite directions, winding roller speed of 450 r/min, rotatable collection roller speed of 35 r/min, and horizontal movement speed of 100 mm/min. To clarify the orientation of these nanofibers, we plated Au/Pd on these samples via a Hummer 6-sputterer device (Anatech, CA, USA). The samples were then imaged, observed, and analyzed via a Hitachi 8230 cold field emission scanning electron microscope (Hitachi, Tokyo, Japan). The average diameter of the NFY-2 was measured via ImageJ software.

Formation of gradient galectin-1 coating on nanofiber yarns 2

The prepared NFY-2 were adhered to square slides (20 mm × 20 mm) with biological glue, fumigated with 75% alcohol for 6 hours, irradiated with ultraviolet light for 1 hour, and soaked in poly-D-lysine (PDL) solution at room temperature for 6 hours. An electrospray strategy capable of creating a unidirectionally linear gradient of active protein on the surface of the receiver device was used to control the distribution of the electrostatic field.[20, 32] Briefly, gelatin was dissolved in acetic acid at a concentration of 6 wt%, and then, galectin-1 at 100 ng/mL was mixed with the gelatin solution at a 1:1 volume ratio. Moreover, to observe the distribution of galectin-1 on NFY-2, 6 mg/mL rhodamine B was added to the mixed solution. The galectin-1 mixture was pumped out at a flow rate of 0.3 mL/h under high pressure at 20 kV via electrospray. The distance between the needle and NFY-2 was 13 cm. Four

customized masks with gaps in the center were placed sequentially on top of the NFY-2, and the last layer of sprays of galectin-1 was collected without using a mask to generate NFY-2 coated by a unidirectionally linear gradient of galectin-1. NFY-2 cells coated with uniform galectin-1 were generated for comparison. The average relative fluorescence intensity of different regions on NFY-2 was measured and plotted via ImageJ software.

Migration, morphology, and viability of neural stem cells and Schwann cells

We investigated the effects of NFY-2 cells coated with a unidirectionally linear gradient of galectin-1 on the migration of NSCs and SCs. NFY-2, nanofiber yarns coated with uniform galectin-1, and blank glass slides served as the control groups. Briefly, polydimethylsiloxane (PDMS) rectangular molds were placed on each sample at a distance of 6 mm from the left edge, leaving a blank area for cell seeding. NSCs and SCs were inoculated at a density of 5×10^5 cells/mL. After cell adhesion was observed, the PDMS molds were removed, allowing NSCs and SCs to migrate. On day 3, the effects of the different groups on the viability of NSCs and SCs were detected via a CCK-8 assay. The morphology and migration of cells stained with Phalloidin-iFluor 488 and DAPI were observed and imaged under a fluorescence microscope (Nikon, Japan). The number of migrated cells was measured from the fluorescence micrographs via ImageJ software.

Determination of the inner fillers and outer walls of the nerve guidance conduits

Schwann cell proliferation and morphology on different nanofibers

The proliferation of SCs cultured on different nanofibers was investigated. The aligned nanofibers, NFY-1 and NFY-2, were attached to circular glass slides with biological glue and then placed in 24-well plates, with the blank glass slides used as the control group (n = 3). All the samples were sterilized with 75% alcohol for 6 hours, treated with ultraviolet light for 1 hour, and washed three times with PBS and DMEM. SCs were then inoculated into 24-well plates at a concentration of 5×10^3 cells/well, and 500 µL of DMEM containing 10% FBS was added to each well. The CCK-8 method was used to detect the effects of the different nanofibers on SC proliferation on days 1, 3, and 5. The cells cultured on day 3 were immobilized and stained with Phalloidin-iFluor 488 and DAPI to observe their morphology via fluorescence microscopy.

Fabrication and characterization of the outer wall

A traditional, single-nozzle electrospinning method was used to deposit nanofibers with random topology on the inner wall of the constructed nerve conduit as the outer wall.[30] PCL was dissolved in HFIP at a concentration of 12% (w/v). The parameters for preparing the random nanofibers were set with a high voltage of 10.5 kV, a flow rate of 1 mL/h, a receiving distance of 15 cm, and a collection time of 5 hours. Imaging and observation of random nanofibers by scanning electron microscopy were carried out.

Neural stem cell and Schwann cell growth in different nerve guidance conduits

Fabrication of hollow polycaprolactone nerve guidance conduits

After determining the structure of the inner wall of the NGCs, we added PCL and ICG at a 120:1 mass ratio into HFIP to produce a PCL mixture with a concentration of 12% (w/v). The PCL/ICG nanofibers were collected continuously and stably via double-nozzle electrospinning. The process lasted for 3 hours, and NFY-1 was obtained as the inner layer of the NGC wall. Immediately afterward, random nanofibers were deposited on NFY-1 as the outer wall of the conduit. The solution was a 12% (w/v) PCL solution without ICG, and the spinning time was 5 hours. On this basis, the bilayer nanofibers were rolled into a tubular shape. When a laser emitter was used, ICG could strongly absorb light energy and convert it into heat energy, so that the overlap of bilayer nanofibers could reach the melting point and weld, thus successfully preparing H-PCL NGCs.[30, 33]

Preparation of filled polycaprolactone nerve guidance conduits

Furthermore, we designed three kinds of filled bionic nerve conduits to study the migration and distribution of NSCs and SCs in 3D structures. The prepared NFY-2 was directly filled into H-PCL NGCs to generate NY-PCL NGCs, and the NFY-2 coated with a unidirectionally linear gradient of galectin-1 was filled into H-PCL NGCs to generate GC-NY-PCL NGCs. HAMA was refilled with the GC-NY-PCL NGCs to generate HA-GC-NY-PCL NGCs.

The distribution and migration of neural stem cells and Schwann cells in different nerve guidance conduits

NSCs and SCs were inoculated into H-PCL NGCs, NY-PCL NGCs, GC-NY-PCL NGCs, or HA-GC-NY-PCL NGCs to assess the distribution and migration of the cells. Specifically, the NGCs were cut into 1 cm lengths and positioned in 24-well plates (n = 3). The samples were subsequently sterilized with 75% ethanol and rinsed with PBS solution. After the samples were soaked in DMEM at 37°C for 2

hours, the NSCs and SCs were inoculated at a density of 1×10^5 cells/mL at the end of the lumen. After 3 hours of cell adhesion, the NGCs were incubated on an oscillator in the incubator. The culture medium was renewed every two days. After 7 days of incubation, the NGCs loaded with cells were fixed with 4% paraformaldehyde at 4°C overnight. Then, frozen sectioning was performed to obtain cross- and longitudinal sections of the NGC-cell composites. Phalloidin-iFluor 488 and DAPI were used to stain the samples for F-actin and nuclei. Next, the distribution and migration of the cells were observed via fluorescence microscopy.

Statistical analysis

The statistical results are expressed as the mean ± standard deviation (SD). To observe the significance of differences among multiple groups, one-way analysis of variance was used. $P < 0.05$ was considered statistically significant.

RESULTS

Determination of galectin-1 concentration

Promotion of Schwann cell *proliferation by different concentrations of galectin-1*

To determine the relative optimal concentration of galectin-1 that can promote the proliferation of SCs, three different concentrations (5, 20, and 50 ng/mL) were selected. As shown in **Figure 1A,** the SCs proliferated well on days 1, 3, and 5 in all the groups. On day 3, the SCs in the 50 ng/mL group proliferated the fastest, significantly different from those in the control and 5 ng/mL groups ($P < 0.01$). On day 5, there was a significant difference between the 50 ng/mL group and the other groups ($P < 0.05$). As shown in **Figure 1D**, there was no difference in the morphology of SCs among all groups on day 3, indicating that the concentration of galectin-1 within a certain range did not affect the morphology of SCs.

Viability and axon growth of PC12 cells promoted by different concentrations of galectin-1

PC12 axon lengths in the 50 ng/mL group were greater than those in the other groups ($P < 0.001$; **Figure 1B**). The viability of PC12 cells on day 4 in each group revealed that the viability of PC12 cells in the 50 ng/mL group was higher than that in the other groups ($P < 0.05$; **Figure 1C**). The corresponding PC12 axon was stained (**Figure 1E**). Combining the above experimental results, the 50 ng/mL concentration was selected for the subsequent study.

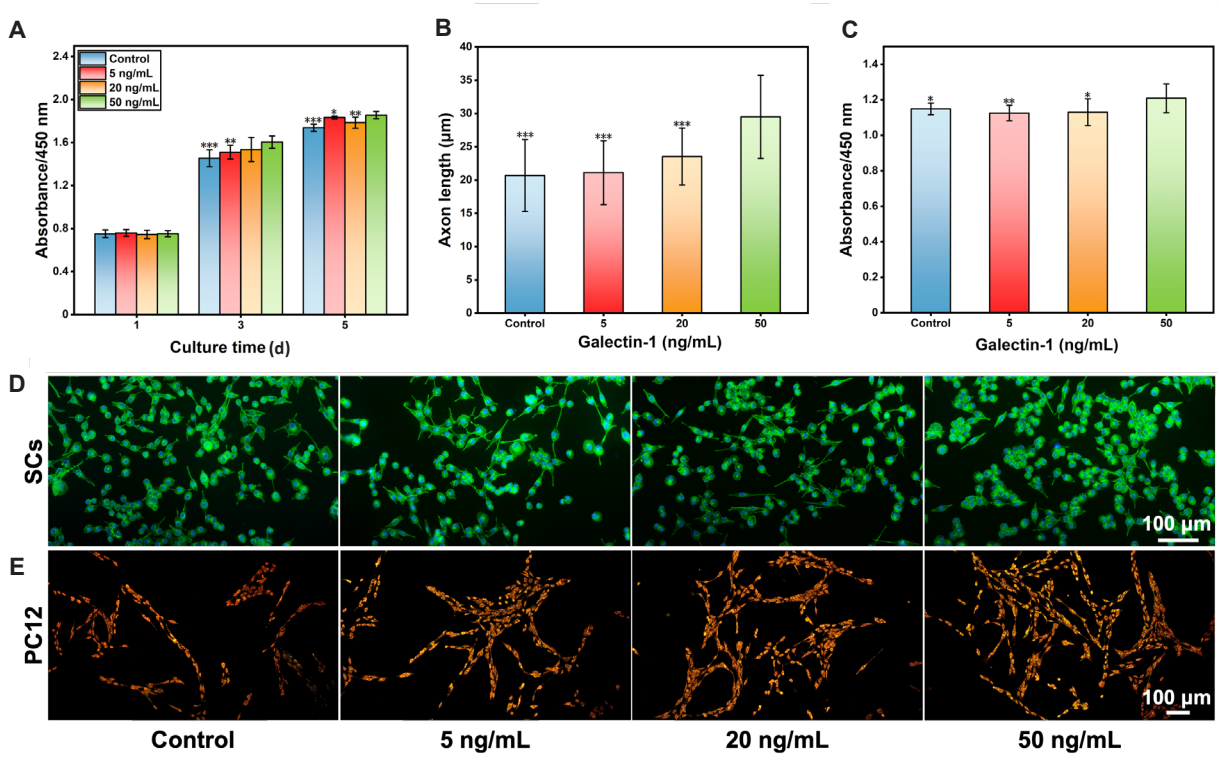

Figure 1: The proliferation and morphology of SCs and viability, morphology, and axon length of PC12 cells cultured with different concentrations of galectin-1.

Note: (A) Proliferation and (D) morphology of SCs after culture in the different groups for 1, 3, and 5 days (A) or 3 days (D). (B, C, E) Statistics of the length (B), viability (C), and morphology (E) of PC12 cells after culture in the different groups for 4 days. *$P < 0.05$, **$P < 0.01$, ***$P < 0.001$, *vs.* the 50 ng/mL group (one-way analysis of variance). SCs: Schwann cells.

Characterization of nanofiber yarns 2 and preparation of gradient coating

NFY-2 was successfully prepared via a commercial instrument. **Figure 2A** shows scanning electron microscopy (SEM) images of NFY-2. The diameter of NFY-2 was controlled to be approximately 192 μm (**Figure 2B**). We then generated NFY-2 coated with a unidirectionally linear gradient of rhodamine B/galectin-1 by controlling the electrostatic field distribution during the electrospray process. Figure 2C shows the relative fluorescence intensities and corresponding fluorescence micrographs of the 5 positions on NFY-2, in order from the beginning to the end. The fluorescence intensity of the highest side at the end was approximately 12 times greater than that of the initial lowest side.

Effects of nanofiber yarns 2 coated with galectin-1 on the migration, morphology, and viability of neural stem cells and Schwann cells

Effects of unidirectional linear gradient galectin-1-coated nanofiber yarns 2 on the migration of neural stem cells and Schwann cells

The migration of NSCs and SCs on glass slides (control group), NFY-2, and NFY-2 coated with uniform or gradient galectin-1 after 3 days of culture is shown in Figure 3A and D. In all groups, the cells migrated to the farthest location. However, the number of migrated cells was significantly higher ($P < 0.05$) in the gradient group than in the other groups (**Figure 3B** and **E**). We divided the migration zone into three regions evenly and measured the number of migrated cells in each region (**Figure 3C** and **F**). In the region (region 1) closest to the seeding area, the migration of NSCs was greater in the gradient group than in the NFY-2 and control groups ($P < 0.05$). Similarly, the number of migrated SCs was significantly higher in the gradient group than in the NFY-2, uniform, and control groups ($P < 0.05$). Moreover, both types of cells in the gradient group tended to migrate to more distant locations than those in the other groups did. This was confirmed by the number of migrated cells in the middle (Region 2) and farthest (Region 3) regions. The number of migrated NSCs in regions 2 and 3 in the gradient group was significantly higher than that in the control and NFY-2 groups ($P < 0.05$). Similarly, the number of migrated SCs in regions 2 and 3 in the gradient group was significantly higher than that in the NFY-2, uniform, and control groups ($P < 0.05$).

Effects of nanofiber yarns 2 coated with galectin-1 on neural stem cell and Schwann cell morphology

The fluorescence micrographs of the morphology of the cells in region 2 from the different groups are shown in **Figure 4A**. The skeletons of the NSCs and SCs presented a stretched morphology, and there were no significant differences among the different yarn groups. However, the NSCs and SCs were arranged randomly in the control group. Overall, the results demonstrated that the NFY-2 coated by a unidirectionally linear gradient of galectin-1 had a remarkable positive effect on cell migration, primarily due to the guidance offered by the biological cue and the orientation of NFY-2, thus inducing the cells to migrate from regions with low galectin-1 content to regions with higher galectin-1 content.

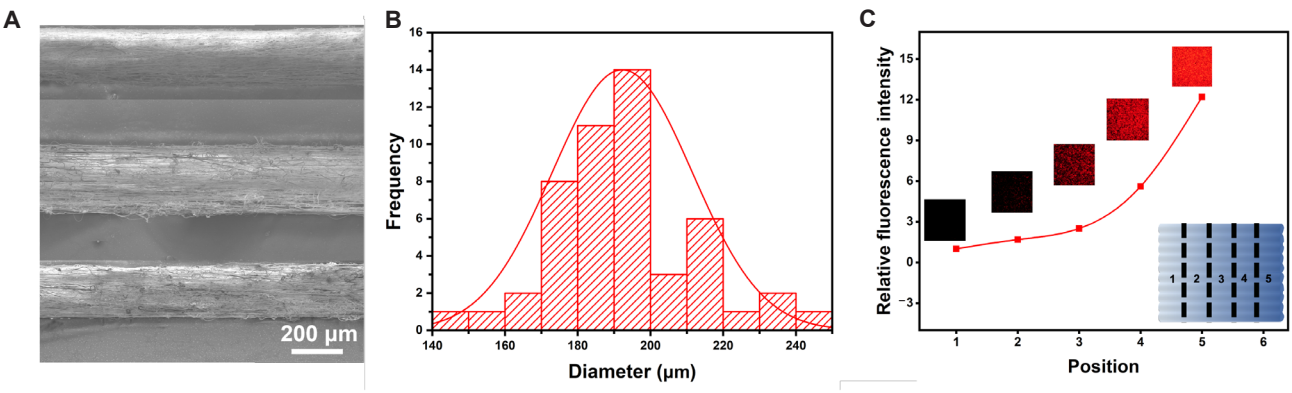

Figure 2: Characterization of the nanofiber yarn (NFY-2) and galectin-1 fluorescence intensity data for NFY-2.
Note: (A, B) Scanning electron microscopy images (A) and diameter distribution of NFY-2 (B). (C) Statistics of the galectin-1 fluorescence intensity of NFY-2.

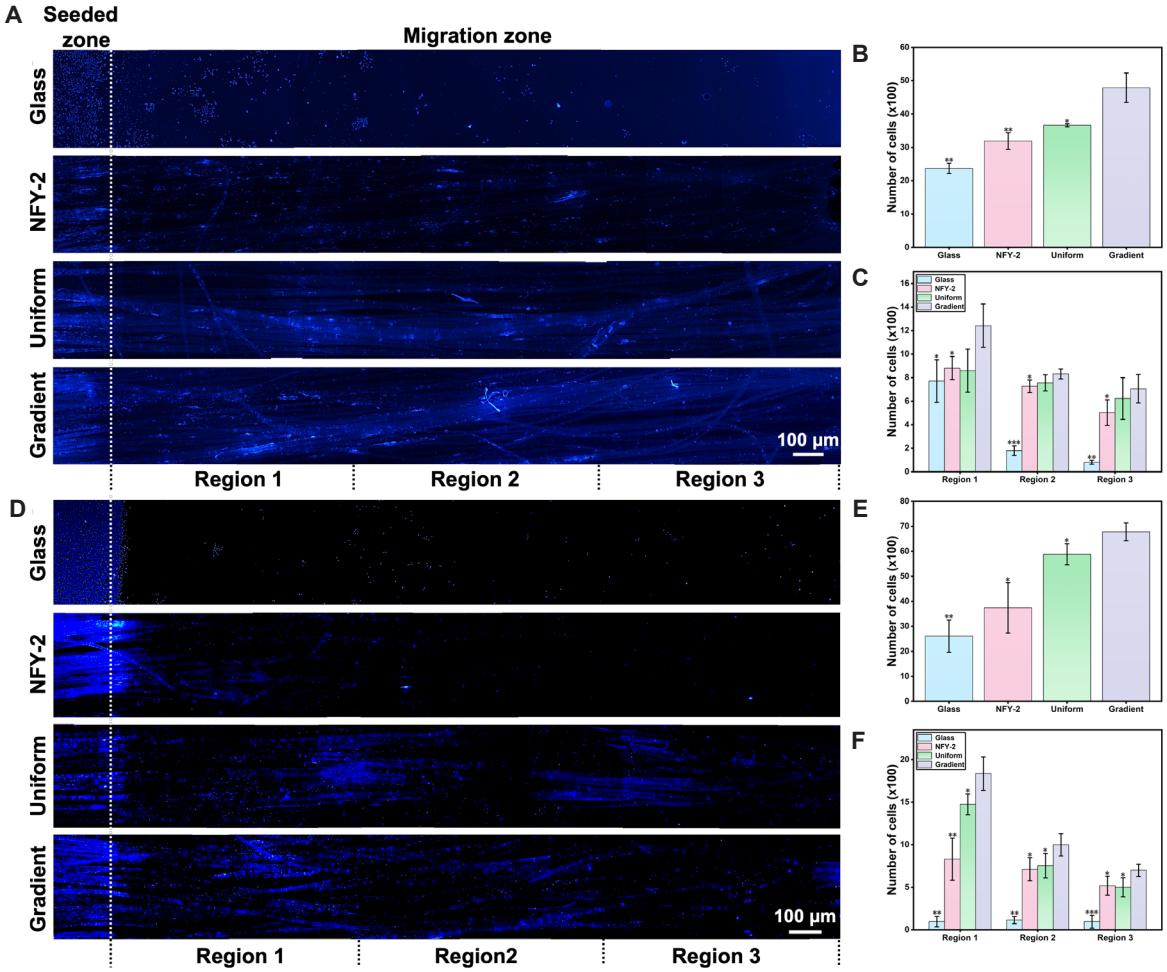

Figure 3: Migration of NSCs and SCs in different groups and statistics of the total number of migrated cells and the number of migrated cells in each region.
Note: (A, D) The migration of NSCs (A) and SCs (D) on the blank glass slides, NFY-2, NFY-2 coated by uniform galectin-1, and NFY-2 coated by unidirectional linear gradient galectin-1. (B, E) Statistics of the total and (C, F) regional numbers of NSCs and SCs after culture for 3 days. *P < 0.05, **P < 0.01, ***P < 0.001, *vs*. gradient group (one-way analysis of variance). NSCs: Neural stem cells; SCs: Schwann cells.

Effect of unidirectional linear gradient galectin-1-coated nanofiber yarns 2 on neural stem cells and Schwann cells

The viability of NSCs and SCs in the control, NFY-2, and NFY-2 groups coated with uniform or gradient galectin-1 on day 3 is shown in **Figure 4B** and **C**. The viability of NSCs and SCs in the gradient groups was the highest, and there was a significant difference compared with the control and NFY-2 groups (P < 0.05). These results indicated that the galectin-1 coating promoted the viability of both NSCs and SCs to a certain extent.

Characterization of nerve guidance conduits

The aligned nanofibers, NFY-2, enlarged NFY-2, and NFY-1 are shown in **Figure 5A**. All the nanofibers were highly oriented. The morphology and orientation of SCs on different nanofibers are shown in **Figure 5B**. Compared with those in the control group, the cells on the aligned nanofibers and NFY-1 adhered and grew in the ordered axial orientation. The distribution of the backbone proteins of the cells was parallel to the orientation of the nanofibers. As shown in Figure 5C, the CCK-8 assay results revealed that the SCs in the four groups proliferated well on days 1, 3, and 5. The proliferation of cells in the NFY-1 group was significantly greater than that in the other groups at all time points (P < 0.05). Compared with that of the control group, the rate of cell proliferation on the aligned nanofibers was significantly greater. The growth of cells in the NFY-2 group exhibited a degree of directionality, albeit to a lesser extent than that observed in the other two experimental groups. The cells in the control group, on the other hand, grew irregularly in all directions.

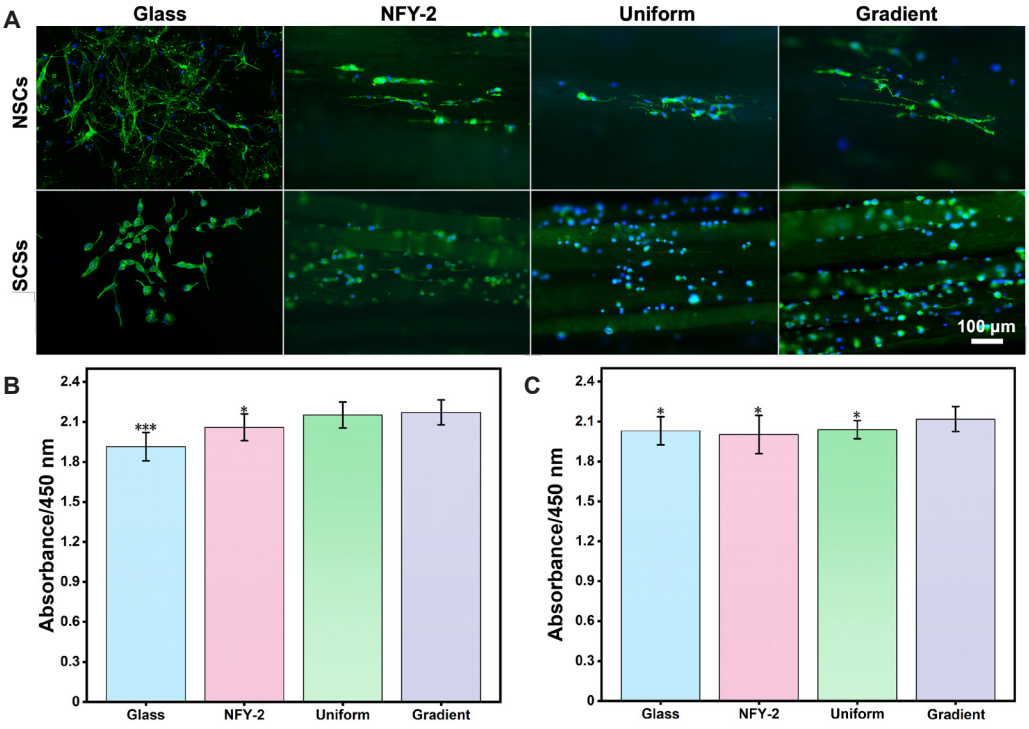

Figure 4: Morphology and viability of NSCs and SCs.
Note: (A) The morphology of NSCs and SCs in migrating region 2 in the different groups. (B, C) Viability of NSCs and SCs on blank glass slides, nanofiber yarns (NFY-2), uniform galectin-1-coated nanofiber yarns, and unidirectional linear gradient galectin-1-coated nanofiber yarns on day 3. *$P < 0.05$, ***$P < 0.001$, *vs*. gradient group (one-way analysis of variance). NSCs: Neural stem cells; SCs: Schwann cells.

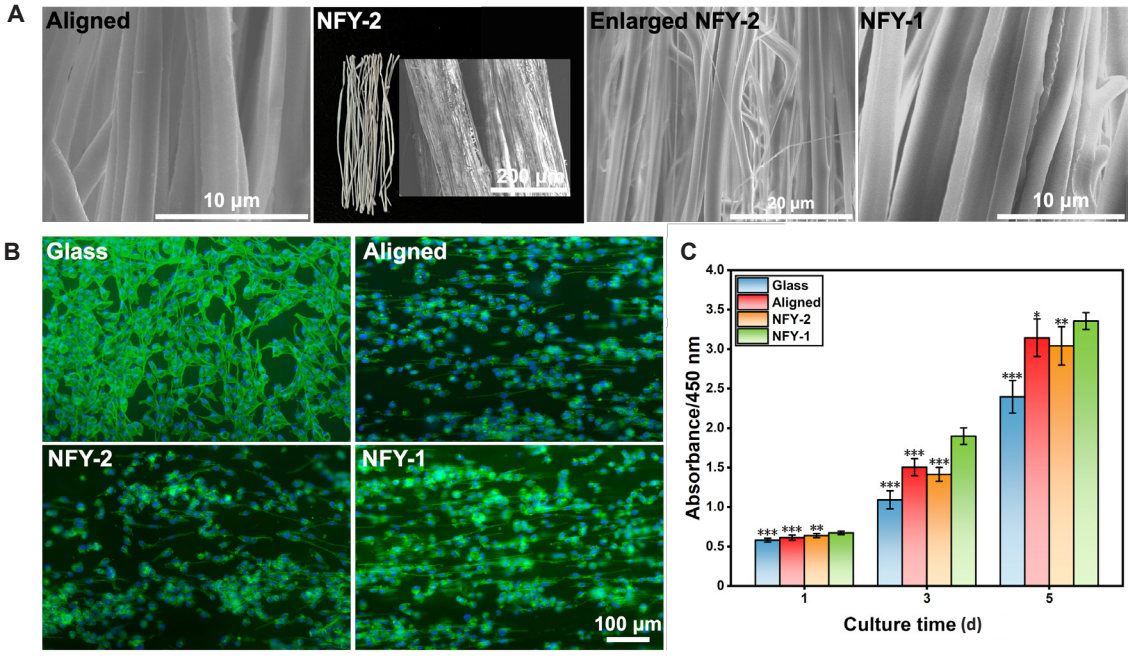

Figure 5: Scanning electron microscopy images of the three nanofibers and the proliferation and morphology of SCs cultured on blank glass slides, aligned nanofibers, nanofiber yarns (NFY-2), and conjugate nanofiber yarns (NFY-1).
Note: (A) Scanning electron microscopy images of aligned nanofibers, NFY-2, partially enlarged view of a single nanofiber yarn, and NFY-1. (B, C) The morphology (B) and proliferation of SCs (C) after culture in the different groups for 3 days (B) or 1, 3, and 5 days (C). **$P < 0.01$, ***$P < 0.001$, *vs*. NFY-1 (one-way analysis of variance). SCs: Schwann cells.

The overall structure and fiber/yarn morphology of H-PCL NGCs, NY-PCL NGCs, GC-NY-PCL NGCs, and HA-GC-NY-PCL NGCs are shown in **Figure 6.** An SEM image of the PCL nanofibers with a random topography is shown in **Figure 6A**. The microstructure of these nanofibers was nonoriented. The diameters of the different NGCs were approximately 2 mm, and there were dozens of NFY-2 in the lumen (**Figure 6B**). SEM images of the NY-PCL NGCs and the single NFY-2 filled in this conduit are shown in **Figure 6C**. **Figure 6D** shows the bilayer structure of the walls of all NGCs, the inner wall (**Figure 6E**) with a conjugate structure, and the outer wall (**Figure 6A**) with a random structure. **Figure 6F** shows an ultradepth field 3D microscope image of H-PCL NGCs. **Figures 6G** and **H** show the overall structure of HA-GC-NY-PCL NGCs and the local SEM images of HA-GC-NY-PCL NGCs. The filled HAMA hydrogel presents a loose porous structure, and NFY-2 is distributed in the porous structure.

Additional Figure 1A–D shows the contact angles of NFY-2 and NFY-2 coated with galectin-1 and NFY-1 on the inner wall of NGCs and random nanofibers on the outer wall of NGCs, respectively. Additional Figure 1E shows that the contact angle of NFY-2 coated with galectin-1 was significantly smaller than that of NFY-2 ($P < 0.05$). This indicated that the hydrophilicity of NFY-2 was improved by the addition of the galectin-1 coating. The cells adhere to hydrophilic surfaces,[34] which may facilitate the adhesion of NSCs and SCs.

Distribution and migration of neural stem cells and Schwann cells in nerve guidance conduits

Figure 7A shows cross-sectional images of the proximal, middle, and distal ends of H-PCL NGCs, NY-PCL NGCs, GC-NY-PCL NGCs, and HA-GC-NY-PCL NGCs and longitudinal images of NSCs 7 days after inoculation. NSCs proliferated only on the inner and outer surfaces of the lumen of H-PCL NGCs, with some regions showing accumulation of NSCs. Many NSCs were located in the proximal lumen of NY-PCL NGCs, GC-NY-PCL NGCs, and HA-GC-NY-PCL NGCs. In the distal lumen of HA-GC-NY-PCL NGCs, the number of NSCs was still evident. **Figure 7B** shows the statistical graph of the number of NSCs in the distal part of the cross-section, indicating that the number of cells in HA-GC-NY-PCL NGCs was the highest and significantly different from that in all other groups ($P < 0.01$). Immunofluorescence images of longitudinal sections revealed NSCs on the luminal surface of H-PCL NGCs, and partial accumulation of NSCs was also observed. Similarly, no significant migration of NSCs was detected within the lumen of the NY-PCL NGCs. However, the production and migration of NSCs were observed on GC-NY-PCL NGCs and HA-GC-NY-PCL NGCs, whereas the number and migration of NSCs within the lumen were significant in HA-GC-NY-PCL NGCs. **Figure 7C** shows the statistical graph of the number of NSCs in the longitudinal section, and the number of cells in the HA-GC-NY-PCL NGCs was the highest and significantly different from that in the other groups ($P < 0.001$).

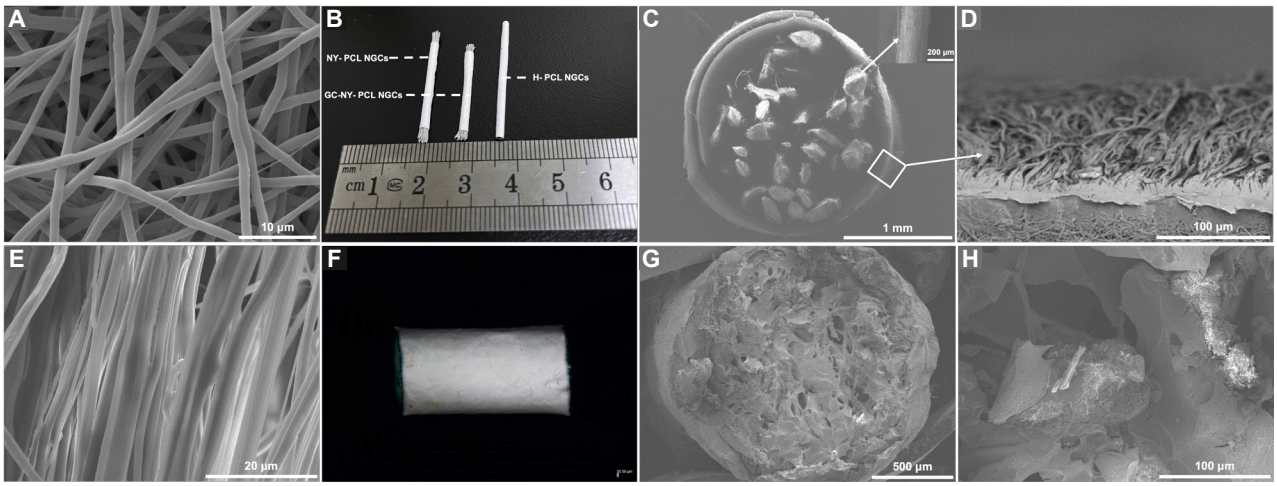

Figure 6: Characterization of NGCs.
Note: (A) SEM images of the outer layer with a random structure. (B) Photographs of H-PCL NGCs, NY-PCL NGCs, and GC-NY-PCL NGCs. (C) SEM images of the NY-PCL NGCs and a single nanofiber yarn. (D) SEM images of the bilayer structure. (E) SEM images of the inner layer with a conjugate structure. (F) Ultra depth-of-field 3D microscope image of H-PCL NGCs. (G, H) SEM images of HA-GC-NY-PCL NGCs and local magnification of hyaluronic acid methacryloyl. GC: Gradient galectin-1; H: hollow; NGCs: nerve guidance conduits; NY: nanofiber yarns; PCL: polycaprolactone; SEM: scanning electron microscopy.

Figure 7D shows cross-sectional and longitudinal staining images of SCs in H-PCL NGCs, NY-PCL NGCs, GC-NY-PCL NGCs, and HA-GC-NY-PCL NGCs. SCs grew and adhered to the inner cavity and outer surface of H-PCL NGCs, and SCs accumulated in some areas. In the lumens of the NY-PCL NGCs, GC-NY-PCL NGCs, and HA-GC-NY-PCL NGCs, SCs grew around the nanofiber yarns. Cross-sections of the HA-GC-NY-PCL NGCs revealed more SCs than other NGCs did. **Figure 7E** shows the statistical graph of the number of SCs in the distal part of the cross-section, indicating that the number of cells in HA-GC-NY-PCL NGCs was the highest and significantly different from that in all other groups ($P < 0.01$). By observing the longitudinal section immunofluorescence images, we also discovered that SCs were generated on the lumen surface of H-PCL NGCs and observed partial accumulation of SCs. Similarly, no significant migration of SCs was detected within the lumen of the NY-PCL NGCs. However, the production and migration of SCs were observed on GC-NY-PCL NGCs and HA-GC-NY-PCL NGCs, whereas the number and migration of SCs within the lumen were evident in HA-GC-NY-PCL NGCs. **Figure 7F** shows the statistical graph of the number of SCs in the longitudinal section, and the number of cells in HA-GC-NY-PCL NGCs was the highest and significantly different from that in all other groups ($P < 0.01$).

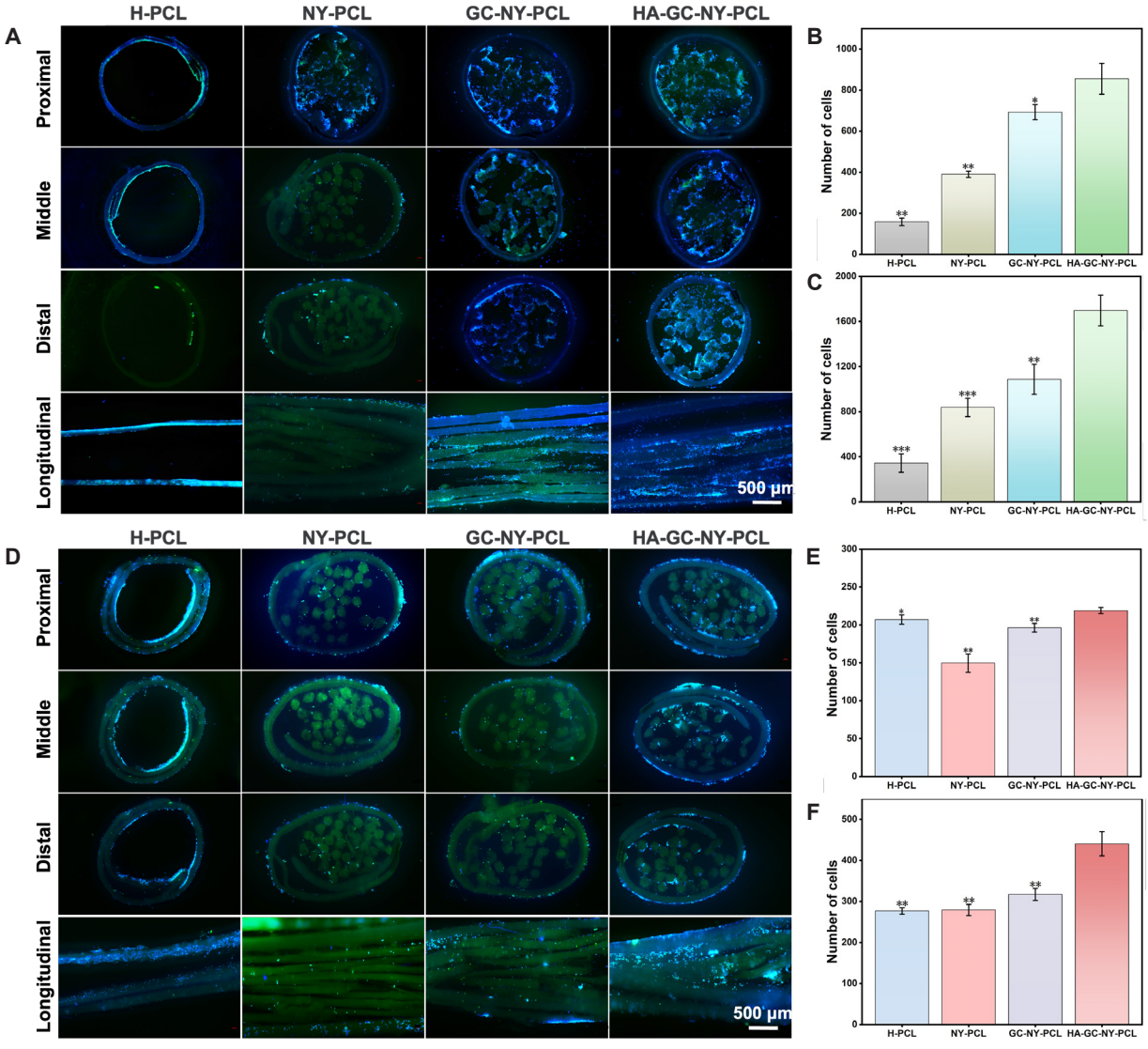

Figure 7: Cross-sectional and longitudinal staining images of NSCs and SCs and their numerical data.
Note: (A, D) The migration of NSCs (A) and SCs (D) on the cross-sectional images of NSCs (A) and SCs in H-PCL NGCs, NY-PCL NGCs, GC-NY-PCL NGCs, and HA-GC-NY-PCL NGCs (D) after 7 days of inoculation in their respective proximal, middle, and distal ends as well as longitudinal staining images. (B, E) The number of NSCs (B) and SCs (E) in the distal cross sections. (C, F) The number of NSCs (C) and SCs (F) in the longitudinal sections. *$P < 0.05$, **$P < 0.01$, *vs*. HA-GC-NY PCL NGCs (one-way analysis of variance). GC: Gradient galectin-1; H: hollow; NGCs: nerve guidance conduits; NY: nanofiber yarns; PCL: Polycaprolactone; SCs: Schwann cells.

Discussion

In this study, the preparation of a unidirectionally linear gradient of galectin-1 coating on NFY-2 was achieved via electrospray. PDL is a highly positively charged amino acid polymer that can bind to any negatively charged protein. Galectin-1 is a negatively charged protein that helps it better adhere to PDL-soaked NFY-2 and facilitates the preparation of the gradient. Additionally, PDL is a nonspecific cell adhesion factor that promotes the adsorption of cells to solid-phase matrices and promotes the adherent growth of cells in cell culture.[35]

The combination of biological cues and topography provided by NFY-2 cells coated with a unidirectionally linear gradient of galectin-1 produced a chemotaxis-inducing effect, which can direct the migration of NSCs and SCs to regions with increased galectin-1 content. The migration of NSCs and SCs after PNI is closely related to the establishment of new nerve loops. The injury site releases a series of growth factors, chemokines, and inflammatory mediators, forming a complex microenvironment that directs NSCs and SCs to migrate toward the injury site. Migrating NSCs can differentiate into new neurons that form synaptic connections with the remaining neurons, restoring nerve conduction function. Moreover, SCs provide nutritional support and protection by forming myelin sheaths to wrap regenerating axons and promote the recovery of nerve function.[36, 37] Therefore, the gradient coating we designed to guide the migration of NSCs and SCs provides a new option for repairing damaged nerves.

Although NFY-2 has the potential to mimic nerve tracts, it still faces the problem of falling apart quickly and not forming when used directly *in vivo*. To overcome this challenge, an empty conduit should be filled with NFY-2. This provides a stable support structure for NFY-2 and helps maintain its positioning *in vivo* to better mimic the function of nerve tracts. The choice and design of the conduit also become critical to ensure that it can have more functionality on the basis of its excellent biocompatibility. Here, we chose NFY-1 as the inner wall of NGCs. The high specific surface area and micro- and nanomorphology of electrospun nanofibers can mimic the extracellular matrix in tissue engineering, which helps promote cell adhesion.[15, 38, 39] In addition, nanofibers with a specific orientation can also induce directional growth of cells.[16] The results of related experiments suggested that NFY-1 is an excellent choice for constructing the inner wall of NGCs, both in terms of its good microstructure orientation and ability to promote the proliferation of SCs as well as directionally induce the growth of SCs. On the basis of our previous study and related literature, PCL nanofibers with random topologies could provide good mechanical strength for nerve conduits.[40] Therefore, we chose it as the outer wall of NGCs.

To explore the potential of 3D-structured NGCs for promoting PNI repair, the prepared H-PCL NGCs, NY-PCL NGCs, GC-NY-PCL NGCs, and HA-GC-NY-PCL NGCs were cocultured with NSCs and SCs to evaluate the migration of these two types of cells inside the NGCs. Although filling NFY-2 into the empty nerve conduit played a supporting role, further filling with HAMA could significantly improve its performance and effect. As a porous 3D network-structured material with high water content and good biocompatibility, HAMA hydrogels can provide a suitable microenvironment for nerve cells.[41] Its injectability allows it to be conveniently filled into the nerve conduit as a liquid, which cross-links under ultraviolet light to form a cured hydrogel, providing stable support for nerve regeneration. NFY-1 and NFY-2 also play good guiding roles simultaneously.[42] However, relying on the topographical cues provided by the scaffold is sometimes insufficient to regulate cell growth and promote tissue regeneration promptly. Specifically, NFY-2 coated with a unidirectionally linear gradient of galectin-1 can improve cell chemotaxis and manipulate the migratory behavior of NSCs and SCs.[43] The experimental results demonstrated that HA-GC-NY-PCL NGCs prepared by electrospinning and light welding were indeed favorable for cell attachment, growth, and migration in terms of function and bioactivity.[33, 44]

The current clinically applied nerve conduits are structurally simple and insufficient to promote the recovery of nerve structure and function.[45] Previous authors have performed numerous studies and attempted to fabricate nerve conduits with multifunctional bionic properties.[46-49] Fibers or hydrogel-filled designs of nerve conduits have been used to increase cell survival and migration. Huang et al. introduced improved gel into collagen-based nerve guides for a rabbit model of delayed repair of tibial nerve defects, showing an excellent supporting effect on axon regeneration.[50, 51] Li et al.[52] fabricated unidirectionally aligned poly(L-lactic acid) nanofiber yarns via a dual spinneret system, which were then put into hollow poly(L-lactide-co-caprolactone) tubes to form nerve conduits. The data revealed that SCs dispersed throughout the lumen and increased well. Compared with the reported filled NGCs, the HA-GC-NY-PCL NGCs had greater strengths in the manufacturing process. NGCs prepared by PCL have been shown to bridge nerve defects to provide access

for nerve regeneration while reducing the risk of infection and improving treatment outcomes.[53] The expected healing time of a nerve injury, however, depends on several factors, including the severity of the injury, the overall health of the patient, and the effectiveness of the treatment approach.[54] PCL nerve conduits degrade *in vivo* over months to years and can support nerve regeneration.[55, 56] Pure PCL nerve conduits for *in vivo* use are prone to collapse, and HAMA filling can achieve a stable structure.[6] In addition, coating NFY-2 with a unidirectionally linear gradient of galectin-1 enhanced the migration of NSCs and SCs. However, many bioactive molecules, such as stromal cell-derived factor-1 and insulin-like growth factor-1′ have been found to play a role in promoting nerve cell migration[57, 58] However, electrospinning coating technology achieves *in situ* delivery and release of bioactive molecules at the injury site, thereby promoting nerve regeneration and repair.[59]

LIMITATIONS

This study has some limitations that should be noted. A long-term efficacy and safety evaluation is needed. Studies may not adequately evaluate the long-term efficacy and safety of HA-GC-NY-PCL NGCs. The absence of long-term data precludes a comprehensive assessment of the practical applications and potential risks associated with HA-GC-NY-PCL NGCs. Future studies should concentrate on the long-term efficacy and safety of HA-GC-NY-PCL NGCs that are required for long-term tracking and evaluation. Importantly, differences between animal models and human applications exist. Subsequent studies may only be conducted in animal models, which are not directly comparable to human applications. The results observed in animal models must fully reflect the potential effects on human patients. It would be beneficial for future studies to conduct clinical trials or further validate the impact of HA-GC-NY-PCL NGCs in human patients, wherever feasible. Material properties and biocompatibility. The properties (such as degradation rate and mechanical strength) and biocompatibility of biomaterials need to be more adequately evaluated. The uncertainty of material properties may affect the performance and effect of nerve conduits. Therefore, future studies should explore the properties of PCL materials and HAMA hydrogels in greater depth and evaluate their influence on nerve conduits.

CONCLUSION

HA-GC-NY-PCL NGCs, which integrate bionic and topological structures and gradient biological cues, offer a potential therapeutic approach to modulate the migration of NSCs and SCs during peripheral nerve injury repair.

Acknowledgments

The authors thank the "Advanced Biomaterials and Regenerative Medicine (ABRM)" Innovation Team supported by the Young-Talent Introduction and Cultivation Plan in the Universities of Shandong Province.

Author contributions

Data curation, conceptualization, investigation, formal analysis, writing - original draft: NL. Methodology, investigation, writing - review & editing: XN. Methodology, investigation, software: XZ. Methodology and investigation: ZZ. Investigation, writing - review & editing: MF. Conceptualization, supervision, writing - review & editing: YW. Resources, conceptualization, methodology, project administration, writing - review & editing, supervision, funding acquisition: TW. All authors approved the final version of the paper.

Conflicts of interest

The authors declare that they have no conflicts of interest.

Additional file

***Additional Figure 1*:** Hydrophilicity of different nanofibers.

REFERENCES

1. Bai J, Yu B, Li C, et al. Mesenchymal stem cell-derived mitochondria enhance extracellular matrix-derived grafts for the repair of nerve defect. *Adv Healthc Mater.* 2024;13:e2302128.
2. Zhu W, Tringale KR, Woller SA, et al. Rapid continuous 3D printing of customizable peripheral nerve guidance conduits. *Mater Today (Kidlington)*. 2018;21:951-959.
3. Ikegami Y, Shafiq M, Aishima S, Ijima H. Heparin/growth factors-immobilized aligned electrospun nanofibers promote nerve regeneration in polycaprolactone/gelatin-based nerve guidance conduits. *Adv Fiber Mater*. 2023;5:554-573.
4. Wu Y, Zou J, Tang K, et al. From electricity to vitality: the emerging use of piezoelectric materials in tissue regeneration. *Burns Trauma*. 2024;12:tkae013.
5. Huang Y, Wu W, Liu H, et al. 3D printing of functional nerve guide conduits. *Burns Trauma.* 2021;9:tkab011.
6. Quan Q, Meng H, Chang B, et al. Novel 3-D helix-flexible nerve guide conduits repair nerve defects. *Biomaterials.* 2019;207:49-60.
7. Fang Y, Wang C, Liu Z, et al. 3D Printed Conductive Multiscale Nerve Guidance Conduit with Hierarchical Fibers for Peripheral Nerve Regeneration. *Adv Sci (Weinh)*. 2023;10:e2205744.

8. Yao L, de Ruiter GC, Wang H, et al. Controlling dispersion of axonal regeneration using a multichannel collagen nerve conduit. *Biomaterials.* 2010;31:5789-5797.
9. Wu T, Li D, Wang Y, et al. Laminin-coated nerve guidance conduits based on poly(l-lactide-co-glycolide) fibers and yarns for promoting Schwann cells' proliferation and migration. *J Mater Chem B.* 2017;5:3186-3194.
10. Wu T, Xue J, Xia Y. Engraving the surface of electrospun microfibers with nanoscale grooves promotes the outgrowth of neurites and the migration of schwann cells. *Angew Chem Int Ed Engl*. 2020;59:15626-15632.
11. Huang Z, Zhang Y, Liu R, et al. Cobalt loaded electrospun poly(ε-caprolactone) grafts promote antibacterial activity and vascular regeneration in a diabetic rat model. *Biomaterials*. 2022;291:121901.
12. Ghomi ER, Lakshminarayanan R, Chellappan V, et al. Electrospun aligned PCL/gelatin scaffolds mimicking the skin ECM for effective antimicrobial wound dressings. *Adv Fiber Mater.* 2023;5:235-251.
13. Liu Y, Guo Q, Zhang X, et al. Progress in electrospun fibers for manipulating cell behaviors. *Adv Fiber Mater*. 2023;5:1241-1272.
14. Camby I, Le Mercier M, Lefranc F, Kiss R. Galectin-1: a small protein with major functions. *Glycobiology*. 2006;16:137R-157R.
15. Kasai K, Hirabayashi J. Galectins: a family of animal lectins that decipher glycocodes. *J Biochem*. 1996;119:1-8.
16. Perillo NL, Marcus ME, Baum LG. Galectins: versatile modulators of cell adhesion, cell proliferation, and cell death. *J Mol Med (Berl).* 1998;76:402-412.
17. Horie H, Kadoya T, Hikawa N, et al. Oxidized galectin-1 stimulates macrophages to promote axonal regeneration in peripheral nerves after axotomy. *J Neurosci*. 2004;24:1873-1880.
18. Sakaguchi M, Okano H. Neural stem cells, adult neurogenesis, and galectin-1: from bench to bedside. *Dev Neurobiol*. 2012;72:1059-1067.
19. Fukaya K, Hasegawa M, Mashitani T, et al. Oxidized galectin-1 stimulates the migration of Schwann cells from both proximal and distal stumps of transected nerves and promotes axonal regeneration after peripheral nerve injury. *J Neuropathol Exp Neurol*. 2003;62:162-172.
20. Zhou Z, Liu N, Zhang X, et al. Manipulating electrostatic field to control the distribution of bioactive proteins or polymeric microparticles on planar surfaces for guiding cell migration. *Colloids Surf B Biointerfaces*. 2022;209:112185.
21. Ji J, Cheng J, Chen C, Lu Y, Chen X, Zhang F. Pirfenidone-loaded hyaluronic acid methacryloyl hydrogel for preventing epidural adhesions after laminectomy. *Drug Deliv Transl Res*. 2023;13:770-781.
22. Wang Y, Lv HQ, Chao X, et al. Multimodal therapy strategies based on hydrogels for the repair of spinal cord injury. *Mil Med Res.* 2022;9:16.
23. Schuurmans CCL, Mihajlovic M, Hiemstra C, Ito K, Hennink WE, Vermonden T. Hyaluronic acid and chondroitin sulfate (meth) acrylate-based hydrogels for tissue engineering: Synthesis, characteristics and pre-clinical evaluation. *Biomaterials*. 2021;268:120602.
24. Mao W, Lee E, Cho W, Kang BJ, Yoo HS. Cell-directed assembly of luminal nanofibril fillers in nerve conduits for peripheral nerve repair. *Biomaterials.* 2023;301:122209.
25. Jin XH, Fang JQ, Wang JG, et al. PCL NGCs integrated with urolithin-A-loaded hydrogels for nerve regeneration. *J Mater Chem B*. 2022;10:8771-8784.
26. Shen J, Wang J, Liu X, et al. In Situ Prevascularization Strategy with Three-Dimensional Porous Conduits for Neural Tissue Engineering. *ACS Appl Mater Interfaces.* 2021;13:50785-50801.
27. Echigo Y, Sugiki H, Koizumi Y, Hikitsuchi S, Inoue H. Activation of RAW264.7 macrophages by oxidized galectin-1. *Immunol Lett.* 2010;131:19-23.
28. Horie H, Inagaki Y, Sohma Y, et al. Galectin-1 regulates initial axonal growth in peripheral nerves after axotomy. *J Neurosci.* 1999;19:9964-9974.
29. Li J, Li X, Li X, et al. Local delivery of dual stem cell-derived exosomes using an electrospun nanofibrous platform for the treatment of traumatic brain injury. *ACS Appl Mater Interfaces.* 2024;16:37497-37512.
30. Liu N, Zhou Z, Ning X, et al. Enhancing the paracrine effects of adipose stem cells using nanofiber-based meshes prepared by light-welding for accelerating wound healing. *Mater Des.* 2023;225:111582.
31. Yu C, Wang T, Diao H, et al. Photothermal-triggered structural change of nanofiber scaffold integrating with graded mineralization to promote tendon–bone healing. *Adv Fiber Mater.* 2023;4:908-922.
32. Xue J, Wu T, Qiu J, Rutledge S, Tanes ML, Xia Y. Promoting cell migration and neurite extension along uniaxially aligned nanofibers with biomacromolecular particles in a density gradient. *Adv Funct Mater.* 2020;30:2002031.
33. Feng Z, Zhang X, Liu N, et al. Promotion of neurite outgrowth and extension using injectable welded nanofibers. *Chem Res Chin Univ.* 2021;37:522-527.
34. Regan LJ, Dodd J, Barondes SH, Jessell TM. Selective expression of endogenous lactose-binding lectins and lactoseries glycoconjugates in subsets of rat sensory neurons. *Proc Natl Acad Sci U S A*. 1986;83:2248-2252.
35. Chen T, Jiang H, Zhu Y, et al. Highly ordered 3D tissue engineering scaffolds as a versatile culture platform for nerve cells growth. *Macromol Biosci.* 2021;21:e2100047.
36. Jenkins PM, Laughter MR, Lee DJ, Lee YM, Freed CR, Park D. A nerve guidance conduit with topographical and biochemical cues: potential application using human neural stem cells. *Nanoscale Res Lett*. 2015;10:972.
37. Yu W, Zhao W, Zhu C, et al. Sciatic nerve regeneration in rats by a promising electrospun collagen/poly(ε-caprolactone) nerve conduit with tailored degradation rate. *BMC Neurosci*. 2011;12:68.
38. Huang R, Hu J, Qian W, Chen L, Zhang D. Recent advances in nanotherapeutics for the treatment of burn wounds. *Burns Trauma*. 2021;9:tkab026.
39. Xiong J, Wang L, Liang F, et al. Flexible piezoelectric sensor based on two-dimensional topological network of PVDF/DA composite nanofiber membrane. *Adv Fiber Mater*. 2024;6:1212-1228.

40. Croisier F, Duwez AS, Jérôme C, et al. Mechanical testing of electrospun PCL fibers. *Acta Biomater*. 2012;8:218-224.
41. Talaei A, O'Connell CD, Sayyar S, et al. Optimizing the composition of gelatin methacryloyl and hyaluronic acid methacryloyl hydrogels to maximize mechanical and transport properties using response surface methodology. *J Biomed Mater Res B Appl Biomater.* 2023;111:526-537.
42. Yang Q, Li J, Su W, et al. Electrospun aligned poly(ε-caprolactone) nanofiber yarns guiding 3D organization of tendon stem/progenitor cells in tenogenic differentiation and tendon repair. *Front Bioeng Biotechnol.* 2022;10:960694.
43. Liu Y, Zhang X, Wang Y, et al. Promoting neurite outgrowth and neural stem cell migration using aligned nanofibers decorated with protrusions and galectin-1 coating. *Chem Commun (Camb).* 2023;59:10753-10756.
44. Wu T, Li H, Xue J, Mo X, Xia Y. Photothermal welding, melting, and patterned expansion of nonwoven mats of polymer nanofibers for biomedical and printing applications. *Angew Chem Int Ed Engl*. 2019;58:16416-16421.
45. Meyer C, Stenberg L, Gonzalez-Perez F, et al. Chitosan-film enhanced chitosan nerve guides for long-distance regeneration of peripheral nerves. *Biomaterials*. 2016;76:33-51.
46. Kim YT, Haftel VK, Kumar S, Bellamkonda RV. The role of aligned polymer fiber-based constructs in the bridging of long peripheral nerve gaps. *Biomaterials.* 2008;29:3117-3127.
47. Lundborg G, Gelberman RH, Longo FM, Powell HC, Varon S. In vivo regeneration of cut nerves encased in silicone tubes: growth across a six-millimeter gap. *J Neuropathol Exp Neurol*. 1982;41:412-422.
48. Xie J, MacEwan MR, Liu W, et al. Nerve guidance conduits based on double-layered scaffolds of electrospun nanofibers for repairing the peripheral nervous system. *ACS Appl Mater Interfaces.* 2014;6:9472-9480.
49. Zhu Y, Wang A, Patel S, et al. Engineering bi-layer nanofibrous conduits for peripheral nerve regeneration. *Tissue Eng Part C Methods.* 2011;17:705-715.
50. Huang Z, Kankowski S, Ertekin E, et al. Modified hyaluronic acid-laminin-hydrogel as luminal filler for clinically approved hollow nerve guides in a rat critical defect size model. *Int J Mol Sci.* 2021;22:6554.
51. Yang S, Zhu J, Lu C, et al. Aligned fibrin/functionalized self-assembling peptide interpenetrating nanofiber hydrogel presenting multi-cues promotes peripheral nerve functional recovery. *Bioact Mater.* 2021;8:529-544.
52. Li D, Pan X, Sun B, et al. Nerve conduits constructed by electrospun P(LLA-CL) nanofibers and PLLA nanofiber yarns. *J Mater Chem B*. 2015;3:8823-8831.
53. Kim J, Park J, Choe G, Jeong SI, Kim HS, Lee JY. A gelatin/alginate double network hydrogel nerve guidance conduit fabricated by a chemical-free gamma radiation for peripheral nerve regeneration. *Adv Healthc Mater.* 2024;13:e2400142.
54. Shan Y, Xu L, Cui X, et al. A responsive cascade drug delivery scaffold adapted to the therapeutic time window for peripheral nerve injury repair. *Mater Horiz.* 2024;11:1032-1045.
55. Dye BR, Youngblood RL, Oakes RS, et al. Human lung organoids develop into adult airway-like structures directed by physico-chemical biomaterial properties. *Biomaterials*. 2020;234:119757.
56. Liang R, Zhao J, Li B, et al. Implantable and degradable antioxidant poly(ε-caprolactone)-lignin nanofiber membrane for effective osteoarthritis treatment. *Biomaterials*. 2020;230:119601.
57. Xie L, Cen LP, Li Y, et al. Monocyte-derived SDF1 supports optic nerve regeneration and alters retinal ganglion cells' response to Pten deletion. *Proc Natl Acad Sci U S A*. 2022;119:e2113751119.
58. Zhang M, An H, Gu Z, et al. Mimosa-Inspired Stimuli-Responsive Curling Bioadhesive Tape Promotes Peripheral Nerve Regeneration. *Adv Mater*. 2023;35:e2212015.
59. Wei Y, Liu Z, Zhu X, et al. Dual directions to address the problem of aseptic loosening via electrospun PLGA @ aspirin nanofiber coatings on titanium. *Biomaterials.* 2020;257:120237.

Date of submission: July 29, 2024
Date of decision: August 29, 2024
Date of acceptance: September 29, 2024
Date of web publication: November 29, 2024